Numerical analysis of rectangular fins in a PCM for low-grade heat harnessing

Mazhar, AR, Shukla, A & Liu, S

Numerical analysis of rectangular fins in a PCM for low-grade heat harnessing

Abdur Rehman Mazhar, Ashish Shukla [*], Shuli Liu

Centre for Research in the Built and Natural Environment, Coventry University, Coventry, CV1 2HF, United Kingdom

A R T I C L E   I N F O

A B S T R A C T

Harnessing waste thermal energy from greywater (GW) in non-industrial buildings is becoming necessary to reduce energy demands, make heating/cooling technologies more efficient and to increase the share of renewables in the consumption. Harnessing this low grade energy to heat incoming cold water (CW) linked with phase change materials (PCMs) would decouple demand and supply along with integrating heat recovery with storage in a single unit, unlike technologies of the past.

Radially installed rectangular copper fins around the GW and CW pipes of such heat exchanger (HE) enhance the thermal conductivity of the PCM which is the biggest obstacle in this high-impulse application, with the flow rate being high only for a short duration of time. Initially an experimental test rig is used to validate a numerical model as the basis of a sensitivity analysis to find the optimum geometric parameters of the finned HE for this application. A 40 × 90 mm fin with a 10 mm pitch provides complete phase change for both melting and freezing in the constrained time duration of 900s. Compared to a non-finned geometry this optimized fin configuration enhances the effective thermal conductivity of the PCM by a factor of 1.38 for melting and 4.75 for freezing. Although the development of buoyancy induced natural convection vortices are inhibited by fins the eventual heat transfer is enhanced due to a lower overall thermal resistance compared to a non-finned configuration. The GW to CW energy transfer efficiency is 72.4% with higher fluid flow temperature increments, compared to only 47.3% for a non-finned version.

1. Introduction

The potential to harness waste heat from grey water (GW) in non-industrial buildings is immense [1]. It is estimated that a mere 10–20% of the original thermal energy is lost before water is converted into GW. Harnessing this heat could save 30–50% in fuel usage in such buildings. In the UK, about 228 GWh of heat has the potential to be harnessed daily which would eventually reduce 6% in annual greenhouse gas emissions. GW heat harnessing would ensure more energy efficient buildings along with reducing heating/cooling demands. Heating up cold water (CW) by harnessing GW heat, linked with Phase Change Materials (PCMs) would not only decouple demand and supply but also integrate heat recovery with storage into a single heat exchanger (HE), unlike technologies of the past [1]. At the same time the evolving concept of low temperature fourth generation district heating grids lack decentralized sources of heat at a large-scale [2]. GW heat harnessing especially in commercial buildings would perfectly suit this requirement along with establishing a more flexible and versatile decentralized heating grid. Although the concept of latent heat storage has gained considerable momentum over the last decades, the principal obstacle is of enhancing the rate of heat transfer [3]. It is especially important in this application since the flow impulse of GW is large, as it has a relatively high flow rate over a short duration of time. For this reason, heat transfer enhancement within the PCM for this GW heat harnessing application is done via rectangular copper fins [4].

In a unique study a Layered Thermal Resistance model was developed to simulate multi-dimensional fins in a PCM [5]. This model can help design an optimal fin arrangement based on the tuning curve/surface, geometry and shape of the layout with the possibility to be integrated in various optimization algorithms unlike typical CFD software's. Sharifi et al. [6] developed a transient numerical model along with analytical correlations to analyse the influence of the number, dimensions and thickness of horizontal plate fins on the melting of a PCM in a 2D rectangular HE. The incorporation of fins accelerated melting with the rate being proportional to the number of fins and their length whilst thickness had the least influence. Since it is an established

* Corresponding author.
  E-mail address: ashish.shukla@coventry.ac.uk (A. Shukla).

fact that fin inclusions in a PCM enhance heat transfer, analysing the effects of a variable sized fin arrangement would be interesting. Based on this research gap, Ji et al. [7] numerically investigated the improvement of a double fin variable length arrangement in internal fluid flow, with a transient simulation. Two unequal parallel horizontal fins were analysed in the melting of RT-42 stored in a rectangular container with a plate heater. A shorter upper fin with a longer lower fin was the optimum solution to maximise buoyancy driven natural convection, reducing the melting time by 25%. Solomon et al. [8] experimentally investigated the effects of adding 8 longitudinal fins during the freezing of a PCM in a cylindrical HE, in order to select the optimum fin height. A reduction in the time of freezing of up to 17.6% was achieved with longer fin heights having an outreach to the extreme ends of the HE container. Similarly heat transfer enhancement with fins is more effective in turbulent flows of the heat transfer fluid (HTF), compared to laminar regimes. In a case study [9], with turbulent flow the PCM melting was 10 times faster and the disparity in the temperature of the PCM was reduced from 15 K to 6 K in comparison to laminar flow. Abujas et al. [10] numerically simulated melting in a 2D model of a tree-shaped branched fin having different materials, in a PCM. It was designed to ensure phase change towards the farthest parts of the HE container, along with a uniform temperature distribution. It was concluded that aluminium fins gave a 20% reduction in melt times to outperform carbon steel fins. The performance was proportional to the amount of fin material used, till an optimum saturation point after which an increment of fin branches produced no additional improvement. At the same time opening a new branch on this fin tree was better than thickening an existing one. Acir et al. [11] performed an analysis of the melting of a PCM using different numbers of fins in a laboratory experiment with artificial solar radiation. It was found that enhancement in melting time was proportional to the number and inversely proportional to the thickness, of fins. Tiari et al. [12] investigated the thermal response and natural convection movement within a PCM having different geometric configurations of a finned heat pipe (HP), in a 2D transient melting simulation. Results showed a direct correlation between the number of HPs and the melting rate whilst the fins ensured a uniform temperature distribution within the PCM. Additionally, numerical simulations of HPs are extremely complex due to the multiple combinations of physical phenomena. Gil et al. [13] conducted an experimental study on a large-scale tank filled with the PCM 'hydroquinone' with 196 square shaped fins. It was concluded, that compared to an arrangement without fins, the effective thermal conductivity increased by 4.11–25.83% depending on the input energy of the HTF. Laing et al. [14] successfully designed radial fins for usage in a large 700 kWh PCM storage unit. The operation of this unit was assessed with various flow rates, pressure and operation conditions of the HTF. It was put forward that the fin design process is subject to continuous optimization in an iterative manner, both in terms of performance and cost.

Most research reporting the usage of fins with PCMs is primarily limited to solar energy storage, passive space heating in buildings, air conditioning, refrigeration, electronic cooling, industrial waste heat recovery and smart textile manufacturing applications [7,12,15]. This paper investigates the novel application of the usage of a finned PCM configuration to harness waste heat from GW as the HTF to transfer to CW as the heat absorbing fluid (HAF).

At the same time most finned-PCM studies provide conflicting outcomes in terms of fin dimensions, including the effects of thickness and pitch [6,16]. This is because the performance of a design is highly dependent on the boundary conditions of the specific application. At the same time, empirical correlations of the performance of finned-PCM applications have not been established till now partly because natural convection is difficult to mathematically predict without incorporating the effects of the geometric layout [6]. This emphasises on the need for an independent study for the dual flow HE, in this application. The fins have to be specifically designed as in a study an improper configuration led to an enhancement of only 2 times compared to a non-finned design,

with a very low cost-to-benefit ratio [9]. Additionally most fin enhancement studies are from the perspective of either melting or freezing with rarely both being analysed simultaneously. This study would assess the performance of a dual purpose single fin arranged on two different pipes, from the perspective of both melting and freezing of the PCM. Similarly the parameter for enhancement for most studies is the phase change time. For this application the parameter of enhancement is the complete phase change fraction, for both melting and freezing in only 900s due to the high impulse rate of this GW heat harnessing application [1].

2. Heat transfer enhancement of PCMs

The heat transfer rate of a PCM can be increased by enhancing its thermal conductivity, the surface area of contact and/or the temperature difference between the PCM with the HTF/HAF [3]. Correspondingly the various techniques are in Fig. 1:

An overview of the techniques are in Table 1:

Hybrid combinations of these enhancement techniques have been reported with the most common being metallic inserts with nano-material composite-PCMs [3,18]. At the same time finned-HPs have proven to be effective as well [3]. Additionally strategies to enhance flow conditions are combined with all other enhancement techniques. A comparative analysis is difficult since the mass and thermal properties of the PCM vary with each technique, while the performance is also application specific [9]. Nevertheless, fins are used to enhance PCM heat transfer in this application, because:

- Particle inserts especially graphite and nanoparticles are the best enhancement techniques [10]. In a comparative study [9], a graphite matrix had the best heat transfer enhancement of 8 times at a cost increment of only about 30%, followed by graphite powder with 3 times and fins with 2 times, compared to a simple PCM configuration. However, particle inserts lack long-term mechanical and thermal stability especially in geometries involving a pipe, having misalignment issues. They cause the PCM to have a heterogeneous structure with uneven thermal characteristics. Their manufacturing and operational costs are high with regular maintenance requirements in indoor building environments, not suitable for this application.
- Although HPs are known to have superior enhancement compared to fins, they are inappropriate for this application. Usually vertical HPs are connected to plate sinks in electronic applications providing a constant heat flux with operational stability [27–29]. In this application, the circular cross-section of a pipe flow makes thermal contact with the HP difficult. Even circular looped HPs are unable to perform consistently due to the transient input heat fluxes. Since this application has a high heat impulse over a short time duration, HPs would be unsuitable as they require a start-up time to function. Additionally HPs increment both the manufacturing and operational costs by manifolds.
- Although encapsulated PCMs advocate in favour of this application due to their compatibility in indoor applications, they considerably reduce the latent heat storage capacity of the PCM. They also lack long-term thermal, mechanical and chemical stability. Operational limitations and void management concerns make them unfitting in this application whilst being expensive and not compact.

In terms of the long-term mechanical, thermal and chemical stability fins are superior especially in piped shell-tube type HEs of this application [5]. At the same time fins enhance both melting and freezing of the PCM since they are conduction dominated, as required [4]. To minimize non-phase changed patches along the outer edges of a HE, long fins are the best approach [10]. Fins are the least expensive with the greatest cost-to-benefit ratio, along with being reliable, compact and the easiest to install [10]. Copper fins are known to perform the best in
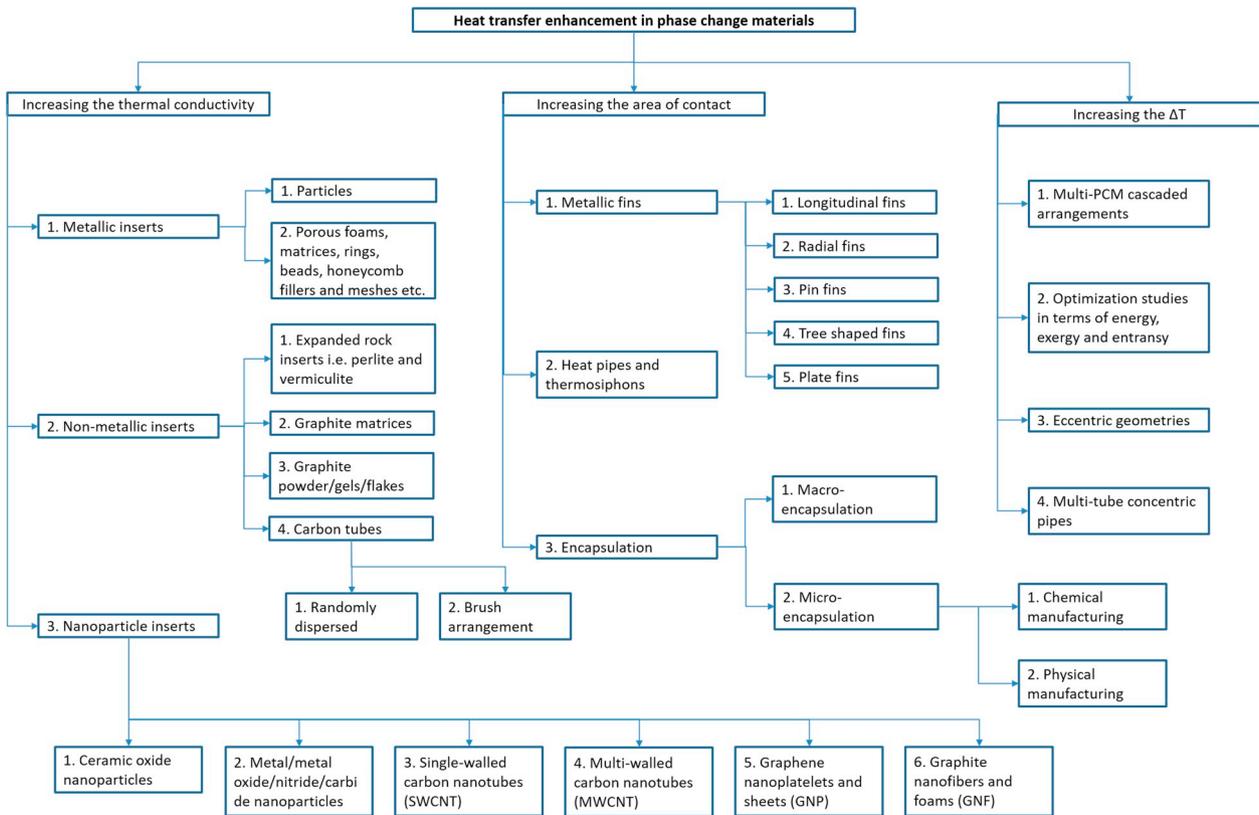
Fig. 1. Techniques to enhance heat transfer in PCMs.

paraffin PCM applications with the least corrosion [6].

3. Numerical model

3.1. Governing equations

There are 7 residuals in this numerical simulation corresponding to 5 different physical laws [30]. For a 3D transient compressible flow, the continuity equation is:

$$\frac{\partial \rho}{\partial t} + \nabla . (\rho v) = 0 \tag{1}$$

As the fluid flow (CW/GW) is modelled as being incompressible (ρ is constant), this mass continuity reduces to a volume continuity balance. The Navier-Stokes momentum equation for a control volume is:

$$\frac{\partial (\rho v)}{\partial t} + \nabla . (\rho v . v) = -\nabla P + \mu \nabla^2 v + \rho g \tag{2}$$

The solution presents the velocity field based on which temperature and pressure is calculated, using the energy equation:

$$\frac{\partial (\rho E)}{\partial t} + \nabla . (v(\rho E + P)) = \nabla . \left(K_{eff} \nabla \mathrm{T} + \left(\mu \left((\nabla v + \nabla v^T) - \frac{2}{3} \nabla . vt \right) . v \right) \right) \tag{3}$$

Due to the 3D fluid flow, the k- ε turbulence model is of importance [31,32]. Two transport equations govern the parameters of the model:

- Turbulent kinetic energy – k

$$\frac{\partial (\rho k)}{\partial t} + \frac{\partial (\rho k v_i)}{\partial x_i} = \frac{\partial}{\partial x_j} \left[\frac{\rho C_\mu \frac{k^2}{\varepsilon}}{\sigma_k} \frac{\partial k}{\partial x_j} \right] + 2\rho C_\mu \frac{k^2}{\varepsilon} E_{ij} E_{ij} - \rho \varepsilon \tag{4}$$

- Rate of dissipation of turbulent energy – ε

$$\frac{\partial (\rho \varepsilon)}{\partial t} + \frac{\partial (\rho \varepsilon v_i)}{\partial x_i} = \frac{\partial}{\partial x_j} \left[\frac{\rho C_\mu \frac{k^2}{\varepsilon}}{\sigma_\varepsilon} \frac{\partial \varepsilon}{\partial x_j} \right] + C_{1\varepsilon} \frac{\varepsilon}{k} 2\rho C_\mu \frac{k^2}{\varepsilon} E_{ij} E_{ij} - C_{2\varepsilon} \rho \frac{\varepsilon^2}{k} \tag{5}$$

The enthalpy method governs the phase change of the PCM. Based on the outcome of the temperatures from the energy equation the non-isothermal enthalpy is updated as [33]:

$$f(x) = \begin{cases} C_s T, \ T < T_s, \ Solid \ phase \\ C_{in} T + \dfrac{L(T - T_s)}{(T_l - T_s)}, \ T_s \leq T \leq T_l, \ Mushy \ region \\ C_l T + L + C_{in}(T_l - T_s), \ T \geq T_l, \ Liquid \ phase \end{cases} \tag{6}$$

The PCM at the phase change interface is in a mushy state, corresponding to the Stefan condition. The temperature and pressure within the PCM are updated, after identification of the phases and interface position.

3.2. Geometry, mesh and solvers

The most common HE layout for a finned-PCM, is a rectangular shell and tube, also suitable for this application [17,18]. It is 180 × 820 × 210 mm containing approximately 20 kg of organic PCM (RT-25) with a melt temperature of 298 K [34], selected with regards to this application, based on a previous study [35]. To maximise heat transfer between the CW and GW, a counter-flow arrangement with 12.7 mm copper pipes is used, linked to fins embedded into the PCM. In PCMs natural convection driven by buoyancy forces due to temperature dependent density and gravitational effects, has an important role during phase change [15]. For this reason the GW pipe is suited to be vertically below the CW pipe, being 150 mm below in this application positioned in the lower half of the rectangular HE to fully exploit the advantages of natural

Table 1
Summary of the techniques of heat transfer enhancement of PCMs.

	Technique	Pros	Cons
1	Metallic inserts	Enhance the thermal response, diffusivity and mechanical rigidity of the PCM. Conduction heat transfer is enhanced to improve both freezing and melting [16]. During freezing the temperature variations within the PCM are minimised.	Are prone to oxidation and corrosion with limited chemical and thermal stability in the long-term. Not all inserts are compatibility with every PCM [17]. The PCM volume change from solid to liquid can destroy foams and matrices or separate the inserts making a heterogeneous mixture with a loss in contact [8]. Voids in pores of structures are an operational concern [9]. Metal foam PCMs are prone to sub-cooling due to increased air bubbles in the pores causing flow resistance [18]. Are not suitable with piped HEs as they cause misalignment, holes and dilatation due to the circular geometry of the pipe [9]. Maintenance issues over the long-term with high costs. Dense foams have a haphazard structure giving the PCM a non-uniform melt temperature and thermal properties whilst hampering natural convection [19]. Has the least surface area to volume ratio increment.
2	Non-metallic inserts	Typically corrosion resistant and robust. Extremely high effective thermal conductivities even along the length of the fibre at about 220 W/(m.K). Lightness due to their low density and a high porosity [9]. Also conduction dominating resulting in improvements in freezing as well. The increment in surface area to volume ratio is high.	Lacks mechanical and thermal stability over the long-term. Complete PCM infiltration not possible with unoccupied pores and air traps making it a heterogeneous mixture with non-uniform thermal properties. Comparatively higher manufacturing, operational and maintenance costs [17]. Carefully designing and controlling the impregnation process in manufacturing is essential [16]. Also hampers natural convection movement in the PCM.
3	Nanoparticle inserts	The increase in conduction enhancement offsets the reduction in convection heat transfer desirable for short time durations. A minimal reduction in the latent heat capacity with the maximum increment in thermal conductivity. High thermal conductivities in the range of 300–3000 W/(m.K) with the best surface area to volume ratios [20].	Greatly enhances melting with less improvements in freezing [20]. During melting separation from the core PCM into big agglomerated clusters causing low freezing enhancement [18]. In the long-term deposits at the bottom of the container due to gravity and density differences of the PCM [21]. Lack of thermal, mechanical and

Table 1 (*continued*)

	Technique	Pros	Cons
			chemical stability over the long-term [17]. Manufacturing and maintenance is complex and expensive. Corrosion of the fin material if not compatible with the PCM [13]. The surface area to volume ratio increment is comparatively lesser from the other techniques.
4	Metallic fins	Conduction dominated improving both freezing and melting [16]. Promotes rapid conduction bringing natural convection much quicker, in melting. The best increment in effective thermal conductivity with the least loss in latent heat capacity. Provides a homogenous temperature distribution without altering the bulk PCM structure [9]. No mechanical or thermal stability concerns over the long-term. Most simplest and economical being the easiest to design, fabricate, install and maintain along with being compact [9,15]. Can easily be coupled with other enhancement techniques.	
5	Heat pipes and thermosiphons	Potential to transfer large amounts of heat over longer distances with a small temperature drop through its length [11]. Transfer of latent heat of the working fluid instead of low density sensible heat [22]. Is mechanically and thermally stable over the long-term. Minimal interference in the core PCM structure proving a homogenous structure, without impeding natural convection. Enhances heat transfer in both freezing and melting. Can easily be coupled in hybrid with other enhancement techniques [23].	Chemical stability of the HP casing with the PCM. Not suitable for piped HEs as the versatility in application usage is limited [24]. Expensive manufacturing and maintenance. Operationally not reliable with PCMs as heat fluxes in the condenser and evaporator vary with time. Start-up from ambient conditions takes at least a few minutes [11]. Occupies considerable volume thereby decreasing the latent heat capacity of the PCM. Has the least surface area to volume enhancement ratio.
6	Encapsulation	Makes PCM usage possible in environments with close human contact including buildings, food storage and medical applications since raw organic PCMs are inflammable [17]. Direct contact of the HTF/HAF with the PCM without contamination and leakage issues [9]. Lightweight and cheap at a macro level[17]. Microencapsulation has the highest surface area to volume ratio. Provides a homogenous bulk structure with uniform thermo-physical properties.	Volume expansion management in the encapsulated core due to ullage compensation, limits the operating conditions [25]. The shell chemically degrades, is vulnerable to mechanical stress and extreme conditions [9]. It absorbs moisture and gets contaminated over the long-term [17]. The thermal stability is limited to 200–5000 cycles only. A uniform non-porous polymeric shell makes manufacturing expensive especially at micro level chemical encapsulation [3]. Has the greatest reduction in latent heat capacity of the PCM. Enhances only conduction heat transfer

Table 1 (*continued*)

Technique	Pros	Cons
		with natural convection almost eliminated being more beneficial in freezing.

convection [18]. In this way a larger portion of the HE and CW pipe are exposed to a higher heat transfer rate. The pipes are laid out horizontally with a length of about 2,280 mm in three straight sections with two bends, whilst being vertically parallel. Rectangular copper fins 170 × 170 mm with a thickness of 1 mm, are fixed on both pipes. Compared with the fin length and number, the influence of thickness on the performance is the least [16]. Closely spaced thin fins are preferred to increase the ratio of the perimeter to the cross-sectional area, with a total of 40 fins having a pitch of 18 mm. The fin thickness of 1 mm is selected based on the cost, ease to manufacture and commercial availability. Thinner fins would be difficult to manufacture and combine with the pipes as the interface contact area would decrease [10]. With the inclusion of such thin fins, the volume and heat capacity loss of the PCM is negligible in this case. Nevertheless in all PCM enhancement techniques, a trade-off has to be achieved in the increment in speed of phase change to that of the decrease in storage capacity due to the reduction in PCM mass [6].

A 3D geometrical model is simulated in the CFD software Star-CCM v12.04. There are four distinct regions merged as a single part: a) the GW fluid domain, b) CW fluid domain, c) solid copper pipe with the rectangular fins and d) the multiphase PCM. The pipes and fins are a single region, with no thermal contact losses between them. An overview of the layout is presented in Fig. 2.

The four regions are discretized using a conformal unstructured polyhedral mesh. For the solid copper domain a surface mesh is developed before a volume mesh, to incorporate the details of the geometry. A set of 9 prism layers are used to model the fluid boundary layers adjacent to the pipe walls. A two layer all 'y+' wall treatment model calculates both the viscous and turbulent effects adjacent to the pipe walls. This model is automatically selected by the standard 'k-ε' turbulence scheme as the CW/GW flow has mixed flow conditions [30]. Based on the targeted 'y+' value and the Reynolds number a primary calculation of the maximum y-value of the first cell height adjacent to the pipe wall, for the prism layer is 1.1 mm.

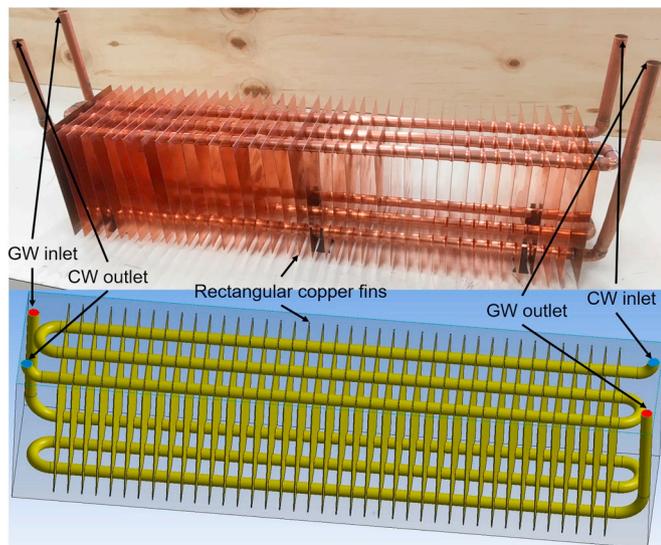An implicit transient simulation for 900s each is performed for both

Fig. 2. Geometric layout of the experimented and simulated model.

melting (GW flow) and freezing (CW flow), of the PCM. The time-step is initially at 0.01s gradually incremented to 1s, as the solution stabilizes and converges to a steady state. Using a High Performance Computer the real-time duration of this simulation is about 48 h owing to the large mesh size and complexity of the solvers. Based on a literature review [1], the mean flowrate of both CW and GW is about 0.1 kg/s. The inlet temperature of the GW is 325 K while that of the CW is 285 K. Due to impurities in the GW, compared to the CW it is modelled as water with a relatively higher constant density of about 1005 kg/m³. The walls of the PCM enclosure are adiabatic with a no-slip condition to eliminate heat losses. The initial temperature of the copper and PCM domain for melting is set at the ambient of 295 K. After the completion of the melting process, the temperature profiles of these two domains are imported as initial conditions into the freezing simulation. The PCM is modelled as Eulerian multiphase using the volume of fluid approach with melting and solidification enabled. Generally liquid PCM, is Boussinesq and Newtonian in nature along with being incompressible with laminar buoyancy motion and negligible viscous dissipation [6]. Amongst the three methods in CFD simulations to model natural convection within a PCM [30], a temperature dependent polynomial density of first-order with gravity enabled, is used in this simulation [34]. Due to the ullage effect the solid phase density is 880 kg/m³ at the solidus temperature of 295.15 K and the liquid phase density is 760 kg/m³ at the liquidus temperature of 299.15 K [34]. The following equation computes this linearly varying PCM density:

$$\rho = 9734.5 - 30 \times T \tag{7}$$

The segregated energy solver is enabled for all four domains of the geometry, as it sequentially solves the governing equations, discretized using the finite volume method. Typically this solver is accurately used for incompressible or mildly compressible flows and is also suited to model convection in PCMs having a low Rayleigh number, as in this application.

3.3. Verification

To ensure that the CFD simulation accurately implements the conceptual framework, a five step verification scheme is implemented [36].

As a first step a mesh convergence study is performed, to ensure spatial discretization convergence. Using four different grid sizes the melt fraction of the PCM is analysed for GW flow. The third largest cell size is considered the most suitable with a difference of less than 3% from the largest configuration. It has about 20 million cells with a reasonable computation time. Secondly, temporal discretization convergence is ensured by varying the initial time-step of the transient solution. With a 0.01s initial time-step, the solution converges with an acceptable real-time computational duration with no loss in accuracy in comparison to lower values. Thirdly, to ensure iterative convergence all 7 residuals corresponding to the governing equations of section 3.1, converge by values of 10^{-2} or lower after the initial transient zone. Due to the nature of the 3D turbulent flow in the corrugated pipes and phase change phenomenon of the PCM, this value is considerably acceptable after the 900s time duration. Fourthly, to verify consistency in the results the simulation for both melting and freezing is repeated 12 times with the same boundary conditions. The confidence level in the results is 99% after assessing three different thermal parameters in the configuration. Finally to theoretically verify the results a sensitivity analysis is performed to consider any abnormalities in the thermal parameters. Variations in the inlet mass-flow rate and temperature of the HTF/HAF are proportional to the amount of phase changed PCM, as predicted in literature [9,18,37]. Similarly the phase change behaviour of the PCM and the magnitudes of the natural convectional currents are within the expected limits, as per literature [11,15]. Additionally a closed system energy and mass balance of the configuration ensure that the governing equations, are verified in the simulation.

3.4. Validation

The numerical model is validated based on experimental data for two different PCMs at two different mass-flow rates for both melting and freezing. The HE of Fig. 2, having the same dimensions and boundary conditions is tested on an experimental rig, in a previous study [37].

Three different variables are compared, with the average deviations from all sets of readings between both datasets enlisted in Table 2:

With the R-squared values between 0.87 and 0.99, and acceptable value differences, the model can be considered as validated [33]. The slight discrepancies between the datasets are due to the following reasons:

- The cumulative uncertainty in the experimental thermocouple readings are 0.4% while 3.15% for the flow meters, coupled with the data loggers. The slow response time of the K-type thermocouples as a solid low-conductivity layer of PCM is developed over them, add to the inevitable systematic errors in the experiment. Similarly the radially inserted probe type thermocouples measure the temperature of the flowing CW and GW in the central portion of the cross-sectional area of the pipe, with less sensitivity to circumferential flow.

- The change in environmental conditions in the experiment also contribute to systematic errors not present in the simulation. The boundary conditions of the experiment fluctuate within tolerable limits while they are modelled as being consistent in the simulation. These differences are amplified in the initial transient zone of the results. As the solution converges to a steady state the differences are much smaller, as highlighted in literature [20].

- The experimental data is recorded every 10s to be interpolated for lower time intervals while the simulation data is more thorough, resulting in slight variations.

- Several assumptions are taken into the simulation which do not completely mimic the experimental test rig. A thermal contact resistance exists between the mechanically fitted fins and pipes in the experiment whilst they are treated as a single domain in the simulation due to computational constraints. At the same time the walls of the HE in the simulation are adiabatic whilst in reality there is some heat loss. In spite of a range of literature available, the flow characteristics for turbulent motion are yet to be fully understood [31, 32]. Mathematically predicting turbulence in CFD simulations has always been a source of error.

- Since the PCM is an amorphous structure, its thermo-physical properties slightly change after every cycle [20]. The amount of disorder in the micro-structure of the PCM is unpredictable at a macro-scale simulation being dependent on the environmental and loading conditions. At the same time, there is not a single consistent phase change temperature as it is dependent on the transient heat flux [38]. For this reason, the PCM close to the pipes and fins exhibit different phase change properties compared to the bulk PCM within the HE. However in the simulation these properties are taken as constant values. Additionally, the errors accumulated in melting are carried forward to the freezing simulation.

4. Results and discussion

With this geometric configuration of the HE, in the 900s time duration only 0.4 of the PCM volume fraction melted while only 0.1 of it froze. Based on this result, it is clear that an optimum fin configuration must be selected to suit this high-impulse application [4]. The height of the fins to the gap between them is the aspect ratio [17]. A large aspect ratio corresponds to high tightly packed fins while a small ratio to short widely spaced fins. Low aspect ratios are effective only near the vicinity of the HTF/HAF while large aspect ratio fins can transfer heat further into the HE quickly [15]. For this GW heat harnessing application involving low time durations a larger aspect ratio is desired for rapid phase change [12]. However, a high aspect ratio configuration also inhibits natural convection flow in the PCM. The fin pitch is inversely proportional to the Rayleigh number, which dictates the amount of convection in the PCM domain [6]. With a lower aspect ratio the thermal resistance is higher but this arrangement does not restrict natural convection [8]. As fin design is application-specific and theoretically unpredictable, the geometrical aspects with respect to the HE determine the performance, which must be investigated. The five parameters to be optimized in this application are labelled in Fig. 3:

Evidently conduction dominated freezing is slower compared to melting [10], hence the design is based on this bottleneck, since the objective is complete phase change for both melting and freezing in 900s. This will maximise latent heat transfer from the PCM to be transferred from the GW to the CW. As the focus is on the optimal development of the fins with the associated pipe configuration, a straight 600 mm length section, is assessed. A model with a fin pitch of 35 mm, width of 60 mm, PCM enclosure length of 10 mm, fin height of 150 mm and a pipe positioning of 15 mm is assessed. The configuration, mesh settings and boundary conditions are similar to the model developed in section 3. Based on this analysis of a smaller length configuration, it can be elongated with both longitudinal and lateral bends as required by installation constraints in the final building environment. Compared to a plane pipe a corrugated pipe with a rib height of 4.5 mm and a pitch of 30 mm is used to enhance internal heat transfer of both the GW and CW flow. This design has been validated and selected based on a previous study [37]. Corrugated pipes are another reason of a smaller 600 mm geometry as a longer configuration would be computationally impossible to generate and solve. The design is optimized based on the GW and CW characteristics of section 3.2. This ensures that the HE is not out of proportion due to an over-design or completely ineffective with an under-design, although it is established that the phase change of a PCM
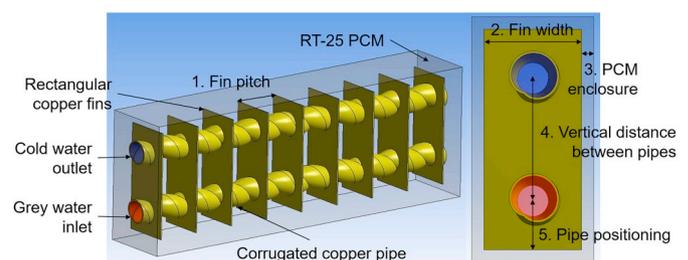

Fig. 3. Configuration of the fins, to be optimized.

Table 2
Difference between the numerical and experimental results.

Operation		Parameter	Linear R-square value	Maximum difference	Mean difference	End value difference
Melting (GW flow)	1	GW (Outlet - Inlet) temperature/K	0.865	0.930	0.599	0.693
	2	Melt fraction of the PCM	0.947	0.186	0.087	0.042
	3	Average temperature of fins/K	0.987	2.380	1.175	2.105
Freezing (CW flow)	1	CW (Outlet-Inlet) temperature/K	0.897	0.783	0.492	0.447
	2	Freeze fraction of the PCM	0.878	0.083	0.055	0.028
	3	Average temperature of fins/K	0.930	4.377	1.871	1.546

is proportional to the mass-flow rate and temperature of the HTF/HAF [18,37].

4.1. Optimized geometry

To determine the optimum geometric parameters of Fig. 3, initially line probes are set adjacent to all three Cartesian directions of the fins, as in Fig. 4:

The results are based on the solid volume fraction of the bottleneck case of freezing after complete melting of the domain, in the 900s duration. Based on the probe perpendicular to the centre of the fin in Fig. 4a, complete freezing of the PCM is observed only until a distance of 10 mm. The second line probe offset by 15 mm being parallel to the width of the fin, depicts that beyond a width of 40 mm from the origin, the amount of frozen PCM decreases in a quadratic behaviour. This is due to the fact that natural convection effects are prominent only in the initial phases of freezing in the vertical orientation and not effective beyond a certain horizontal distance. This is proven by the fact that within the 40 mm fin width, phase change initiates after about 200s whilst increasing in time at widths beyond this. Finally in Fig. 4c, a probe measures the solid volume fraction in a vertical direction adjacent to the upper edge of the fin. It is observed that beyond 5 mm, the PCM is not completely frozen. Based on the completely frozen PCM in the directions of the line probes the dimensions are selected. However to assess the appropriate height of the fin and pipe positioning, the fin temperature contours for both melting and freezing, are in Fig. 5:

There exists a steep temperature gradient along the height of the fin of about 25 K for melting and 20 K for freezing. Freezing has a lesser gradient primarily because less PCM is frozen in 900s, minimising the ability of the fin to conduct and propagate heat. It is observable from Fig. 5, that beyond 2/3rd of the height, in both processes, the fin is unable to effectively conduct heat as the temperature gradient drops rapidly. However the magnitude of this gradient increases rapidly in the vicinity of the pipes, for both cases. For freezing the temperature at the extreme end of the fin, is well above the liquidus temperature resulting in no phase change at all, in this position. The temperature variation after 900 s at these extreme ends of the fin for both cases is extremely low in comparison to the initial temperature. Therefore it can be deduced that if the height is reduced by at least 2/3rd of the 150 mm, the fin would be more effective in providing complete phase change with a uniform temperature gradient. Additionally at a radius of about 5–10 mm from the pipe edge, the temperature profile of the fin is consistent for both cases. For this reason, it is viable to increase the pipe positioning from the fin edge to 20 mm instead of the 15 mm. This would also facilitate in promoting a more uniform temperature distribution within the fin.

For such thin fins it is presumed that the temperature is uniform across their 1 mm thickness [16]. Normally thicker fins have more uniform temperature profiles along their height while thinner fins exhibit a temperature gradient, as evident in this application [18]. However thicker fins have a higher response time, to take longer for temperature variations. Consequently, the 5 optimized parameters are

in Table 3:

These are a single discrete set of parameters amongst numerous combinations resulting in complete melting and freezing. Since these parameters are interdependent on each other, a direct optimization study is not possible. Similar to this sensitivity analysis, a combination has to be constructed to be systematically analysed.

4.2. Fin vs non-finned comparison

Based on the configuration of Table 3, a finned geometry is compared to a non-finned version as in Fig. 6, with the same dimensions and boundary conditions.

With the 60 fins of 10 mm pitch on the 600 mm length corrugated pipe the increment in surface area of the copper domain is by a factor of 13.75 compared to the non-finned version. Similarly the amount of volume occupied by the fins is 1.78×10^{-4} m^3. This corresponds to a surface area to volume increment ratio of 5607. The increment in the mass is only 1.45 kg proving that the cost-to-benefit ratio with fins is enormous. Aluminium fins would have been even lighter but with a lesser thermal conductivity and an increase in contact losses as the pipe and fins would be of different materials with dissimilar thermal expansion coefficients. The percentage reduction in the PCM mass with fins is only 6.7% and the latent storage capacity loss is about 25 kJ.

As per the initial objective of maximising heat transfer, the amount transferred to the PCM in the 900s is about 360 kJ with an average heat flux rate of 0.40 kW for melting and 340 kJ from the PCM at 0.38 kW for freezing, in the finned configuration. Compared with the non-finned version these values correspond to 260 kJ with 0.29 kW for melting and 71 kJ with 0.08 kW for freezing.

The ratio of the actual to the maximum theoretical capacity in lieu of both sensible and latent heat is widely used to categorize the exergetic efficiency of a PCM based HE [14]. If the dead state is at the ambient of 295 K, the maximum theoretical limit of heat transfer is when the PCM approaches the GW temperature while melting and the CW temperature while freezing, defined as:

$$\eta_{exergy} = \frac{\text{Actual heat transferred to PCM}}{\text{Maximum theoratical heat trasnferred to PCM}}$$
$$= \frac{mC_p\left(T_{final} - T_{initial}\right) + \lambda mL}{mC_p\left(T_{GW/CW} - T_{initial}\right) + mL} \tag{8}$$

This would include sensible heat transfer outside the PCM phase change temperature range of 295.15–299.15 K and latent heat transfer within. Melting beyond 299.15 K would result in superheated liquid PCM while freezing below 295.15 K would result in subcooled solid PCM.

Based on the end values, this exergetic efficiency for the finned version in melting is 91.3% while that of freezing is 85.6%. These values are considerably high yet below the maximum since there is always an upper limit to sensible heating, as per the second law of thermodynamics. The same values for the non-finned version are 57.1% and 16.8%, proving the effectiveness of this optimum fin configuration.
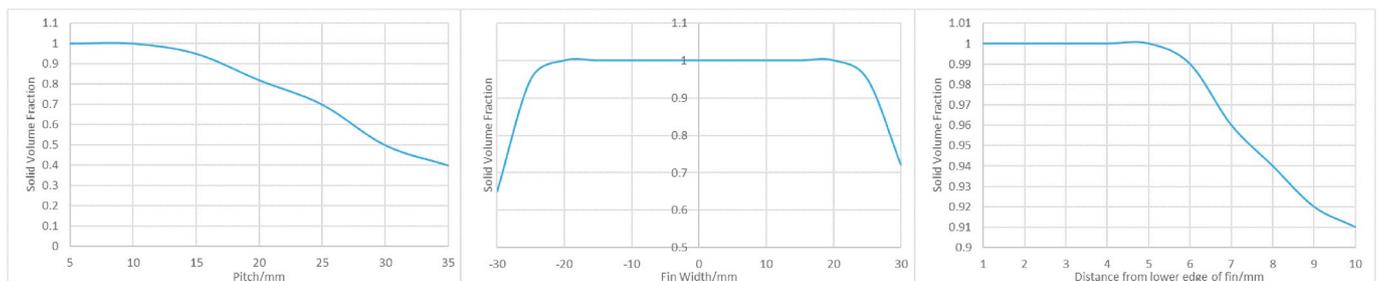

Fig. 4. Solid volume fractions at line probes a) perpendicular to the fin (z-axis) b) parallel to the fin width offset by 15 mm (x-axis) c) adjacent to the upper horizontal edge of the fin (y-axis), for freezing.
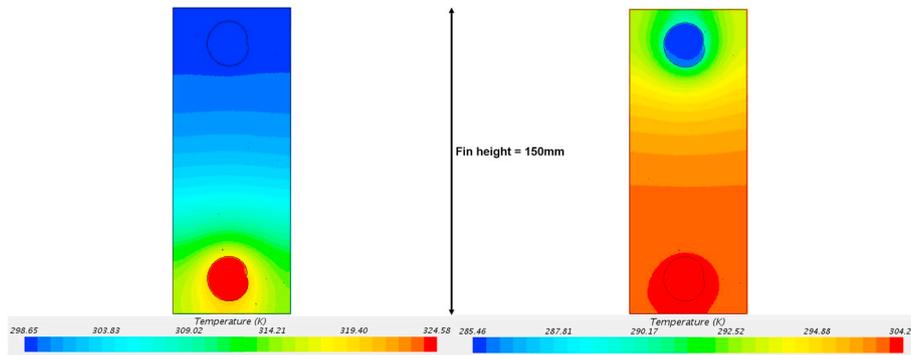
Fig. 5. Assessment of the fin height based on the temperature gradient for a) melting b) freezing, of the PCM.

Table 3
Optimized geometric parameters of the fins with respect to the HE.

	Parameter	Value/mm
1	Fin pitch	10
2	Fin width and height	40 × 90
3	PCM enclosed on sides of fin	5
4	Vertical height between pipes	50
5	Pipe position with respect to fin edge	20

Similarly the Stefan number for the end values is defined as:

$$St = \frac{Sensible\ heat\ transfer}{Latent\ heat\ transfer} = \frac{mC_p\left(T_{final} - T_{initial}\right)}{\lambda mL} \qquad (9)$$

It is the ratio of the sensible to latent heat transferred by the PCM with an ideal value close to zero. For the finned version the Stefan number for both melting and freezing is 0.24. However in the non-finned version it is 0.1 for melting while 0.24 for freezing. In the finned geometry there is considerable sensible heating during melting since the optimization is done based on the bottleneck case of freezing. Comparatively in the non-finned version most heat transfer is latent

without complete phase change. In optimum configurations both values should be equal for complete phase change, as in this case [18].

Although the enhancement in melting is noticeable, the improvement in freezing is substantial with the optimized fin configuration. A widely used criteria in PCM based HEs with enhanced heat transfer techniques, is the effective thermal conductivity [13], defined as the ratio of heat transferred with and without fins [18]. In this application this ratio is 1.38 for melting and 4.75 for freezing. The reason for this increment is depicted in the resistance diagram of Fig. 6:

Typically, the response time of PCMs is extremely slow becoming a hurdle especially in electronics and space applications unlike in solar thermal and building applications, where a response time of a few hours is acceptable [14], due to which fins are extremely important. Fins decrease the overall thermal resistance [17] and compared to a non-finned version, two additional flow paths for the heat to propagate are provided. The total thermal resistance of a parallel arrangement is much less compared to a series arrangement resulting in an overall lower thermal resistance to heat flow.

As a follow on to Fig. 5, the temperature profiles of the fin in the optimized geometry are in Fig. 7:

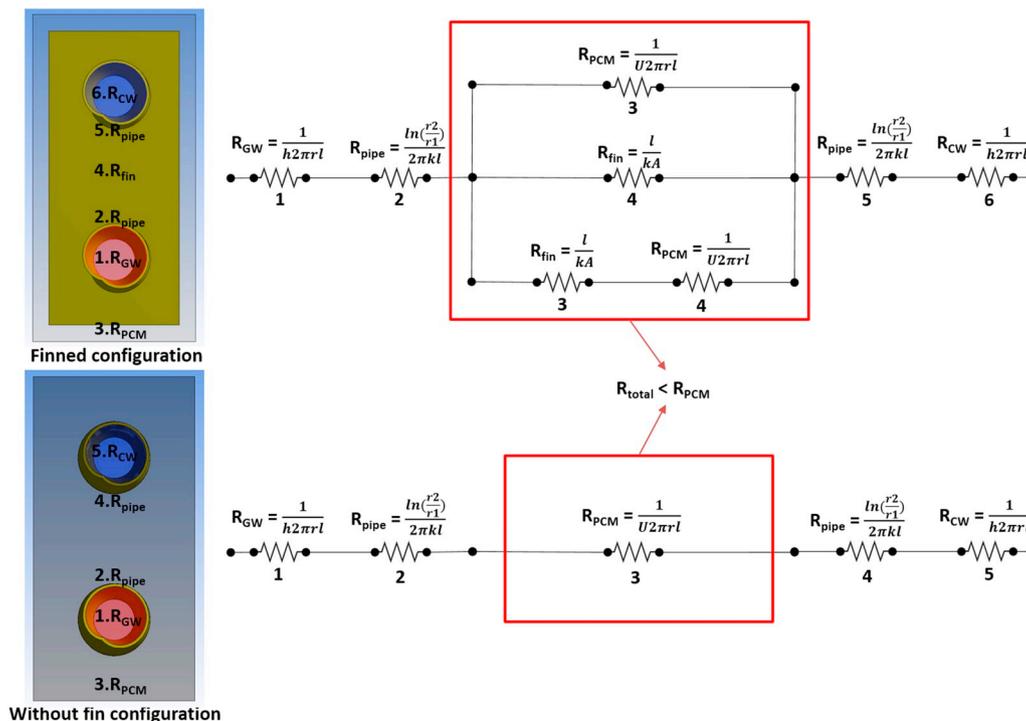Comparatively heat propagation across the height of the fin is more

Fig. 6. Thermal resistance diagram for the finned and non-finned configurations.

uniform with a lower temperature gradient of 13 K for melting and 9 K for freezing. At the same time the temperature of the entire fin in freezing is below the solidus temperature resulting in complete freezing. In the case of melting, the fin propagates heat even more efficiently being considerably above the liquidus temperature. Consequently, complete PCM melting with uniform temperature profiles are visible in the temperature contour compared to the non-finned configuration of Fig. 8:

For the finned configuration, the PCM in the vicinity of the GW pipe has an average temperature close to the fluid while the PCM close to the CW pipe is at a relatively lower temperature, but still in liquid phase. This is because the hot convectional currents originate from the bottom to the top transferring heat along the height of the fins. Comparatively in the non-finned configuration PCM melting occurs only on the edges of the GW pipe with the remaining being at a uniform temperature below the liquidus temperature. After the melting process, the temperature profiles of the PCM and copper domain are imported into the freezing simulation. The resulting temperature contours for freezing have a similar trend as in Fig. 9:

Similar to the melting phenomena, fins ensure complete freezing of the PCM with the temperature differential from top to bottom only at about 5 K. Since the PCM in the vicinity of the GW pipe was initially at a much higher temperature after the melting process, it remains so but in solid phase. On the other hand the non-finned configuration has negligible freezing only near the lower edges of the CW pipe. The thickness of the frozen layer is even lesser compared to the phase changed layer in melting. This is because the solid frozen layer around the edges acts as a heat insulator having an extremely low thermal conductivity, making freezing much slower compared to melting.

Since the layout of the configuration is based on the bottleneck case of freezing, there is considerable sensible heat transfer in melting compared to freezing, as depicted by the transient phase change plots of Fig. 10:

At about 320s complete melting of the PCM occurs after which the heat transferred is sensible. As expected [11], the heat transfer curve can be divided into three parts; pre-phase change sensible, phase change latent and post-phase change sensible heat transfer, clearly visible in the finned freezing plot of Fig. 10b. This corresponds to three distinctive regimes involving slow initial convection followed by a sharp change to faster conduction domination for the remaining duration completed by a slow conduction heat transfer finish [6]. During the freezing process, initially convection in the liquid PCM is followed by conduction as the temperature falls below the liquidus temperature. Fins enhance this second conduction regime in the PCM resulting in a much steeper gradient. In the non-finned configuration this regime is non-existent, eventually which makes the difference towards complete phase change.

Additionally, the reason for an improved melting time in the PCM, is that fins enhance conduction to initiate convection at a much earlier stage. Although fins are a hurdle to the flow of natural convection currents, but the offset in convection hindrance is smaller than the
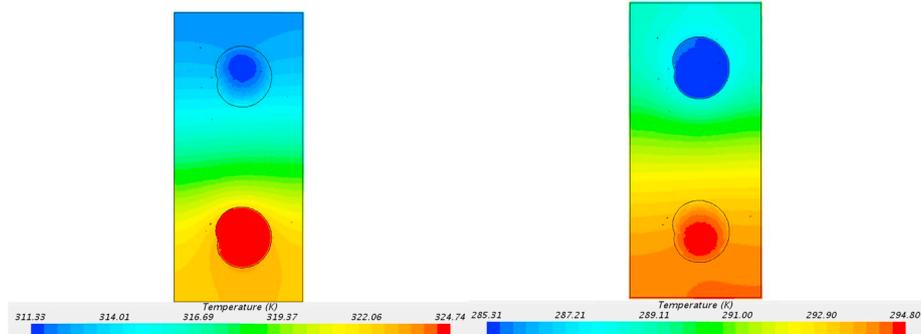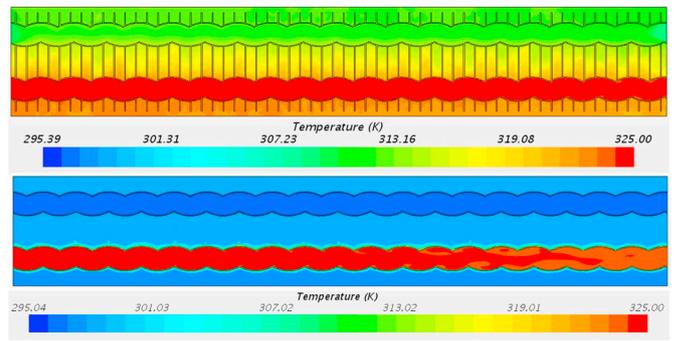

Fig. 8. Cross-sectional view of the temperature profile of the a) finned b) non-finned, configurations for melting.
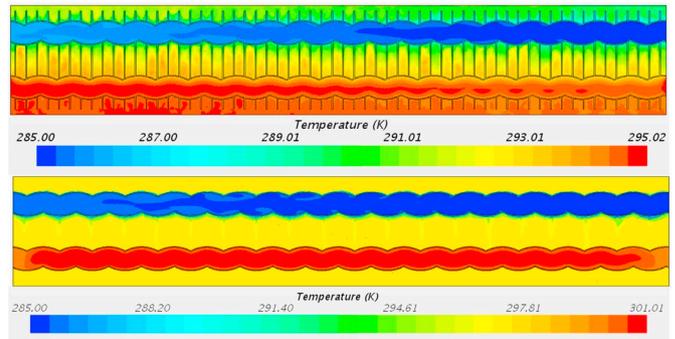

Fig. 9. Cross-sectional view of the temperature profile of the a) finned b) non-finned, configurations for freezing.

increment in conduction propagation, resulting in an overall improvement. Natural convection is initiated in the PCM as the Rayleigh number exceeds 10^5 [30] and doubles the melting rate compared to only heat transfer via conduction [18]. The thermal conductivity of liquid PCM is even lower than that of the solid phase, making natural convection propagation in melting extremely important [26]. It clearly plays an important role in both the configurations as visible in the cross-sectional velocity contour along the length, for melting in Fig. 11:

The volume averaged velocity for the finned configuration is about 0.004 m/s and 0.008 m/s of the non-finned version. Nevertheless, the finned configuration sustains convection to a reasonable extent eventually resulting in complete melting in the 900s duration. The finned configuration inhibits convectional currents in the central portion of the contour while only allowing them to freely develop on the outskirts of the HE. In the non-finned version, the convection vortices are originating across the entire length, as there are no restrictions to the movement. In a similar study[15], it was also observed that small vortices form only around the fins and HTF pipe, even in the early stages
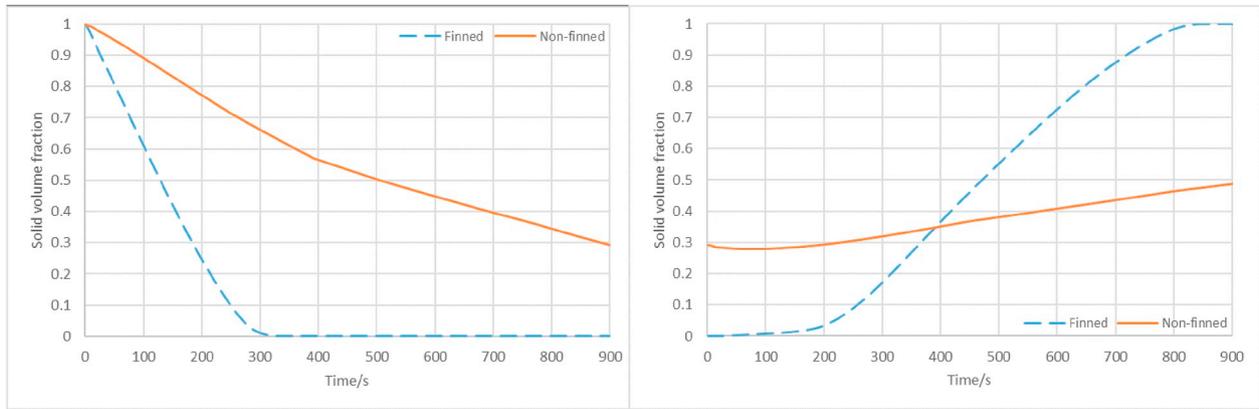

Fig. 7. Temperature profile of the fin for the optimized geometry for a) melting b) freezing, of the PCM.

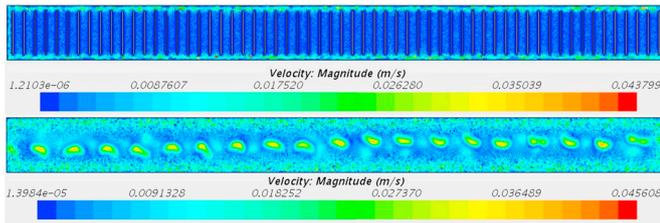**Fig. 10.** Phase change profile for a) melting b) freezing, of the PCM.

Fig. 11. Cross-sectional view of the velocity profile of the a) finned b) non-finned configurations.

of melting. With the passage of time these vortices increase in size along with moving vertically upwards due to buoyancy. They are visible in the streamlines of the liquid PCM for both configurations in Fig. 12:

In the non-finned configuration the vortices can be seen originating from the GW pipe moving towards the top of the HE. Comparatively, for the finned version there is no organised bulk movement in the centre, only towards the edges of the HE. Most of the movement in the remaining PCM is haphazard with limited velocities.

Another parameter of interest is the change in temperature of the incoming fluids, as the CW would be eventually used for heating in non-industrial applications. The inlet temperature of the GW is 325 K and that of the CW is 285 K, as in section 3.2. An overview of the outlet temperature profiles for the 900s duration, are in Fig. 13:

In Fig. 13a, the GW loses less heat compared to the non-finned configuration after 600s. The reason for this is correlated to Fig. 10a. After 300s the entire PCM melts and after 600s, the sensible temperature of the PCM domain also increases to its maximum limit. As there is no more capacity for heat to propagate from the GW, it loses lesser heat compared to the non-finned configuration after 600s. However in the non-finned configuration propagation of heat is consistent during the 900s, but the net heat transfer is lesser in comparison. As the design is

based on the bottleneck case of freezing, this trend is not evident in Fig. 13b. The maximum heat transfer potential of the PCM is not reached in freezing unlike in melting, resulting in a consistently higher CW temperature compared to the non-finned case.

Initially the temperature differentials are high for both flows eventually reaching a steady state to asymptotically decrease to the inlet temperatures. The bell-shaped curves of Fig. 13, are typical to this application due to the variations in the thermal diffusivity of the copper and PCM [37]. The average GW outlet temperature for the entire time duration for melting in the finned configuration is 322.1 K while that for the non-finned version is 323.1 K. Similarly the average CW outlet temperature for the finned configuration is 287.1 K while that for the non-finned version is 285.9 K. Although the temperature differential is not significant but the short length of this layout must be considered. In real practical HEs with longer pipe lengths this differential would amplify to enable the HE to be a decentralized heat source, as envisioned [2]. The effectiveness of this HE is based on the average heat transfer between both fluids defined as [39]:

$$\eta_{effectiveness} = \frac{Heat\ absorbed\ by\ CW}{Heat\ trasnferred\ from\ GW} = \frac{(T_{out} - T_{in})}{(T_{in} - T_{out})} \quad (10)$$

For the finned configuration the effectiveness is 72.4% while for the non-finned version it is 47.3%. At the same time, the temperature differentials in the fluid flows for the non-finned configuration are much lower.

5. Conclusion

Harnessing heat from GW to CW via a PCM HE is a novel approach to decouple demand and supply whilst integrating thermal recovery along with storage into a single unit. The enhancement in heat transfer to the PCM is investigated via radially installed rectangular fins on the pipes. A numerical model is validated with an experimental setup with an
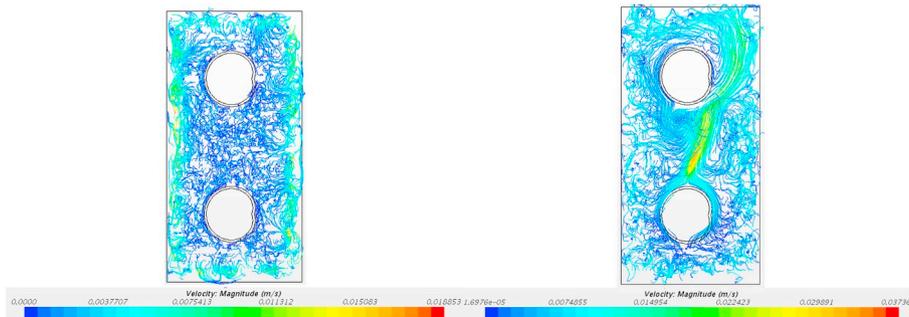

Fig. 12. Propagation of natural convection vortices in the a) finned b) non-finned configuration.
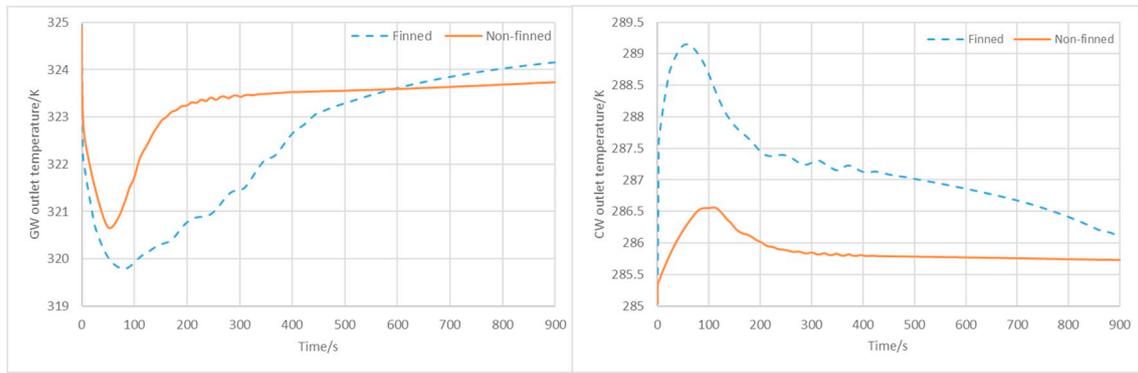
Fig. 13. Outlet temperature profile for the a) GW b) CW, flows.

average R-square value 0.92, between both datasets. Based on which an optimum configuration of 40 × 90 mm copper fins with a 10 mm pitch are developed, to maximise latent heat transfer between the fluids and complete phase change for both melting and freezing of the PCM. Compared to a configuration without fins, this layout enhances the effective thermal conductivity in melting by 1.38 and freezing by 4.75 times. At the same time the finned configuration has an equal Stefan number for both melting and freezing of 0.24 compared to an unbalanced number for the non-finned version. It is also observed that heat transfer is enhanced in spite of the average velocity of the convectional currents decreasing by half in the finned configuration. Fins are a hurdle to the free flow of these currents especially in this application, as they have a high aspect ratio. Nevertheless there is a net increment in heat transfer as the improvement in initial propagation of heat via conduction is higher than this hindrance in convective heat transfer. The finned configuration has a heat transfer efficiency of 72.4% from the GW to CW compared to only 47.3% for a simple version. The results signify that the developed layout has a higher energy and exergetic efficiency along with successfully decoupling CW and GW supply with demand, as was the objective [1].

It is recommended that, based on the layout of this unit module the overall economic and technical performance of a holistic HE, be analysed especially with respect to a case study. At the same time the investigation of using multi-cascaded PCM arrangements to further improve heat transfer, would be interesting.

Acknowledgement

Nomenclature

GW	Grey water
CW	Cold water
PCM	Phase change material
HE	Heat exchanger
HTF	Heat transfer fluid
HP	Heat pipe
HAF	Heat absorbing fluid
ρ	Density in kg/m^3
t	Time in s
v	Velocity in m/s
P	Pressure in Pa
μ	Dynamic viscosity in Pa.s
g	Acceleration due to gravity in m/s^2
E	Energy in J
K_{eff}	Effective thermal conductivity in W/(m.K)
T	Temperature in K
ε	Rate of dissipation of turbulence energy in W
x	Position in m
C_μ	σ_k, σ_ε, $C_{1\varepsilon}$, $C_{2\varepsilon}$ Constants of the turbulence model dependent on iterations and conditions
E_{ij}	Component of the rate of deformation
C	Specific heat capacity in kJ/(K.kg)
L	Specific latent heat capacity in J/kg
y^+	Dimensionless wall treatment height
η	Efficiency
m	Mass in kg
λ	Phase change fraction
St	Stefan number
h	Heat transfer coefficient due to convection in W/(m^{2}K)

r   Radius in m
l   Length in m
k   Thermal conductivity in W/(m.K)
U   Overall heat transfer coefficient in W/(m.K)
A   Area in m^2
R   Thermal Resistance in K/W

Abbreviations
s   Solidus
l   Liquidus
in   Interface
p   Pressure

References

[1] A.R. Mazhar, S. Liu, A. Shukla, A key review of non-industrial greywater heat harnessing, Energies 11 (2018), https://doi.org/10.3390/en11020386.

[2] A.R. Mazhar, S. Liu, A. Shukla, A state of art review on the district heating systems, Renew. Sustain. Energy Rev. 96 (2018) 420–439, https://doi.org/10.1016/j.rser.2018.08.005.

[3] Y.B. Tao, Y.L. He, A review of phase change material and performance enhancement method for latent heat storage system, Renew. Sustain. Energy Rev. 93 (2018) 245–259, https://doi.org/10.1016/j.rser.2018.05.028.

[4] F.P. Incropera, D.P. DeWitt, T.L. Bergman, A.S. Lavine, Fundamentals of Heat and Mass Transfer, 2011.

[5] C. Pan, S. Hoenig, C.H. Chen, S. Neti, C. Romero, N. Vermaak, Efficient modeling of phase change material solidification with multidimensional fins, Int. J. Heat Mass Tran. 115 (2017) 897–909, https://doi.org/10.1016/j.ijheatmasstransfer.2017.07.120.

[6] N. Sharifi, T.L. Bergman, A. Faghri, Enhancement of PCM melting in enclosures with horizontally-finned internal surfaces, Int. J. Heat Mass Tran. 54 (2011) 4182–4192, https://doi.org/10.1016/j.ijheatmasstransfer.2011.05.027.

[7] C. Ji, Z. Qin, S. Dubey, F.H. Choo, F. Duan, Simulation on PCM melting enhancement with double-fin length arrangements in a rectangular enclosure induced by natural convection, Int. J. Heat Mass Tran. 127 (2018) 255–265, https://doi.org/10.1016/j.ijheatmasstransfer.2018.07.118.

[8] G.R. Solomon, R. Velraj, Analysis of the heat transfer mechanisms during energy storage in a Phase Change Material filled vertical finned cylindrical unit for free cooling application, Energy Convers. Manag. 75 (2013) 466–473, https://doi.org/10.1016/j.enconman.2013.06.044.

[9] K. Merlin, D. Delaunay, J. Soto, L. Traonvouez, Heat transfer enhancement in latent heat thermal storage systems: comparative study of different solutions and thermal contact investigation between the exchanger and the PCM, Appl. Energy 166 (2016) 107–116, https://doi.org/10.1016/j.apenergy.2016.01.012.

[10] C.R. Abujas, A. Jové, C. Prieto, M. Gallas, L.F. Cabeza, Performance comparison of a group of thermal conductivity enhancement methodology in phase change material for thermal storage application, Renew. Energy 97 (2016) 434–443, https://doi.org/10.1016/j.renene.2016.06.003.

[11] A. Acır, M. Emin Canlı, Investigation of fin application effects on melting time in a latent thermal energy storage system with phase change material (PCM), Appl. Therm. Eng. 144 (2018) 1071–1080, https://doi.org/10.1016/j.applthermaleng.2018.09.013.

[12] S. Tiari, S. Qiu, M. Mahdavi, Numerical study of finned heat pipe-assisted thermal energy storage system with high temperature phase change material, Energy Convers. Manag. 89 (2015) 833–842, https://doi.org/10.1016/j.enconman.2014.10.053.

[13] A. Gil, G. Peiró, E. Oró, L.F. Cabeza, Experimental analysis of the effective thermal conductivity enhancement of PCM using finned tubes in high temperature bulk tanks, Appl. Therm. Eng. 142 (2018) 736–744, https://doi.org/10.1016/j.applthermaleng.2018.07.029.

[14] D. Laing, T. Bauer, N. Breidenbach, B. Hachmann, M. Johnson, Development of high temperature phase-change-material storages, Appl. Energy 109 (2013) 497–504, https://doi.org/10.1016/j.apenergy.2012.11.063.

[15] M. Kazemi, M.J. Hosseini, A.A. Ranjbar, R. Bahrampoury, Improvement of longitudinal fins configuration in latent heat storage systems, Renew. Energy 116 (2018) 447–457, https://doi.org/10.1016/j.renene.2017.10.006.

[16] A.M. Abdulateef, S. Mat, J. Abdulateef, K. Sopian, A.A. Al-Abidi, Geometric and design parameters of fins employed for enhancing thermal energy storage systems: a review, Renew. Sustain. Energy Rev. 82 (2018) 1620–1635, https://doi.org/10.1016/j.rser.2017.07.009.

[17] A.S. Fleischer, Thermal Energy Storage Using Phase Change Materials Fundamental and Applications, 2015, https://doi.org/10.1007/97-3-319-20922-7.

[18] Z. Khan, Z. Khan, A. Ghafoor, A review of performance enhancement of PCM based latent heat storage system within the context of materials, thermal stability and compatibility, Energy Convers. Manag. 115 (2016) 132–158, https://doi.org/10.1016/j.enconman.2016.02.045.

[19] R. Senthil, M. Cheralathan, Natural heat transfer enhancement methods in phase change material based thermal energy storage, Int. J. Chem. Res. 9 (2016) 563–570.

[20] C. Wang, T. Lin, N. Li, H. Zheng, Heat transfer enhancement of phase change composite material: copper foam/paraffin, Renew. Energy 96 (2016) 960–965, https://doi.org/10.1016/j.renene.2016.04.039.

[21] K.W. Shah, A review on enhancement of phase change materials - a nanomaterials perspective, Energy Build. 175 (2018) 57–68, https://doi.org/10.1016/j.enbuild.2018.06.043.

[22] N.R. Rudonja, M.S. Komatina, G.S. Živković, D.L. Antonijević, Heat transfer enhancement through pcm thermal storage by use of copper fins, Therm. Sci. 20 (2016) s251–s259, https://doi.org/10.2298/TSC1150729136R.

[23] H. Shabgard, M.J. Allen, N. Sharifi, S.P. Benn, A. Faghri, T.L. Bergman, Heat pipe heat exchangers and heat sinks: opportunities, challenges, applications, analysis, and state of the art, Int. J. Heat Mass Tran. 89 (2015) 138–158, https://doi.org/10.1016/j.ijheatmasstransfer.2015.05.020.

[24] N. Sharifi, T.L. Bergman, M.J. Allen, A. Faghri, Melting and solidification enhancement using a combined heat pipe, foil approach, Int. J. Heat Mass Tran. 78 (2014) 930–941, https://doi.org/10.1016/j.ijheatmasstransfer.2014.07.054.

[25] C.W. Robak, T.L. Bergman, A. Faghri, Enhancement of latent heat energy storage using embedded heat pipes, Int. J. Heat Mass Tran. 54 (2011) 3476–3484, https://doi.org/10.1016/j.ijheatmasstransfer.2011.03.038.

[26] P. Sivasamy, A. Devaraju, S. Harikrishnan, Review on heat transfer enhancement of phase change materials (PCMs), Mater. Today Proc. 5 (2018) 14423–14431, https://doi.org/10.1016/j.matpr.2018.03.028.

[27] A. Ambirajan, A.A. Adoni, J.S. Vaidya, A.A. Rajendran, D. Kumar, P. Dutta, Loop heat pipes: a review of fundamentals, operation, and design, Heat Tran. Eng. 33 (2012) 387–405, https://doi.org/10.1080/01457632.2012.614148.

[28] B.W. Hu, Q. Wang, Z.H. Liu, Fundamental research on the gravity assisted heat pipe thermal storage unit (GAHP-TSU) with porous phase change materials (PCMs) for medium temperature applications, Energy Convers. Manag. 89 (2015) 376–386, https://doi.org/10.1016/j.enconman.2014.10.017.

[29] R. Yogev, A. Kribus, PCM storage system with integrated active heat pipe, Energy Procedia 49 (2013) 1061–1070, https://doi.org/10.1016/j.egypro.2014.03.115.

[30] SIEMENS, Star CCM+ Documentation v12.04. Plano, 2017.

[31] P.G. Vicente, A. García, A. Viedma, Experimental investigation on heat transfer and frictional characteristics of spirally corrugated tubes in turbulent flow at different Prandtl numbers, Int. J. Heat Mass Tran. 47 (2004) 671–681, https://doi.org/10.1016/j.ijheatmasstransfer.2003.08.005.

[32] B. Mohammadi, O. Pironneau, Analysis of the K-Epsilon Turbulence Model. Pris: Chichester; Paris: Wiley; Masson, 1994.

[33] V. Alexiades, A.D. Solomon, Mathematical Modeling of Melting and Freezing Processes, Taylor & Francis, Washington, 1993.

[34] Rubitherm Technologies GmbH, Data Sheet RT25. Berlin, 2016.

[35] A.R. Mazhar, S. Liu, A. Shukla, An optimizer using the PSO algorithm to determine thermal parameters of PCM: a case study of grey water heat harnessing, Int. J. Heat Mass Tran. 144 (2019) 118574, https://doi.org/10.1016/j.ijheatmasstransfer.2019.118574.

[36] M. Marini, R. Paoli, F. Grasso, J. Periaux, J.A. Desideri, Verification and validation in computational fluid dynamics, JSME Int. J. Ser. B Fluids Therm. Eng. 45 (2002) 15–21, https://doi.org/10.1299/jsmeb.45.15.

[37] A.R. Mazhar, S. Liu, A. Shukla, Experimental study on the thermal performance of a grey water heat harnessing exchanger using Phase Change Materials, Renew. Energy 146 (2019) 1805–1817, https://doi.org/10.1016/j.renene.2019.08.053.

[38] M. Iten, S. Liu, A. Shukla, Experimental validation of an air-PCM storage unit comparing the effective heat capacity and enthalpy methods through CFD simulations, Energy 155 (2018) 495–503, https://doi.org/10.1016/j.energy.2018.04.128.

[39] A. Al-Abidi, S. Mat, K. Sopian, Y. Sulaiman, A. Mohammad, Heat transfer enhancement for PCM thermal energy storage in triplex tube heat exchanger, Heat Tran. Eng. 37 (2016) 705–712, https://doi.org/10.1080/01457632.2015.1067090.